Experimental study of an asymmetric Stockbridge damper

Giacomo Bacci[1], Ole Øiseth[1], Øyvind W. Petersen[1], Vincent Denoël[2]

[1]*NTNU, Trondheim, Norway, giacomo.bacci@ntnu.no*
[2]*ULiège, University of Liège, Liège, Belgium*

SUMMARY:
Hanger vibrations are a known issue in many modern suspension bridges, often linked to innovative hanger designs. To address these vibrations, Stockbridge dampers—originally used in high-voltage cables—have been adapted for structural engineering. However, frequent cases of damper failure have been reported globally, with the root causes still undetermined. This study investigates an asymmetric Stockbridge damper installed on the hangers of a long-span suspension bridge in northern Norway. Experimental testing was conducted on the complete damper as well as on its separated top and bottom masses to assess its performance across various vibration frequencies and amplitudes. The findings provide insights into the damper's behavior, which can support numerical modeling and inform future design strategies for Stockbridge dampers in structural applications. This work contributes to optimizing damper installation and enhancing the effectiveness of vibration mitigation in bridge structures.

Keywords: Stockbridge, experimental setup, nonlinear device

1. SETUP DESCRIPTION

A Stockbridge damper comprises two flexible messenger cables connecting weighted masses to a central clamp attached to the vibrating structure. When the structure vibrates, the masses oscillate, deforming the messenger cables. Damping arises from static hysteresis due to Coulomb (dry) friction between the cable's individual wires undergoing bending deformation (N. Barbieri and R. Barbieri, 2012). In this study, the damper was designed to mitigate vortex-induced vibrations on the Hålogaland Bridge in northern Norway. To resemble the field installation position, in the experimental setup the damper is positioned vertically, supported by two bending load cells, and connected to a horizontal slider, as illustrated in Fig. 1. Each mass is equipped with two IEPE accelerometers to capture lateral and rotational motion, while an additional accelerometer on the slider records the clamp motion. The damper is excited using a modal vibration shaker (APS 420), which provides monoharmonic excitation at constant and sweep frequencies between 3 and 35 Hz. Following IEEE 664-1993 (IEEE Standards Committee, 1993), the velocity amplitude of the clamp motion was maintained constant during experiments. Field measurements on the Hålogaland Bridge indicated velocity amplitudes between 0.01 m/s and 0.05 m/s, while the IEEE guide recommends 0.1 m/s. Numerical models for Stockbridge dampers in the literature (N. Barbieri and R. Barbieri, 2012; Foti and Martinelli, 2018) were identified for half-dampers and then applied to symmetric dampers by doubling the output force for a given input clamp motion. With this modeling approach in mind, the damper is tested in halves, with the top half shown in Fig. 5a and the bottom half in Fig. 5b. The sensor layout remains consistent with the full damper configuration. The main geometric characteristics of the damper are summarized in Table 1.

Table 1. Geometric parameters of the Hålogaland Stockbridge dampers.

Upper mass [kg]	**Lower mass** [kg]	**Total mass** [kg]	**Length messenger cable** [mm]	**Diameter messenger cable** [mm]
4.9	8.0	14	250	16

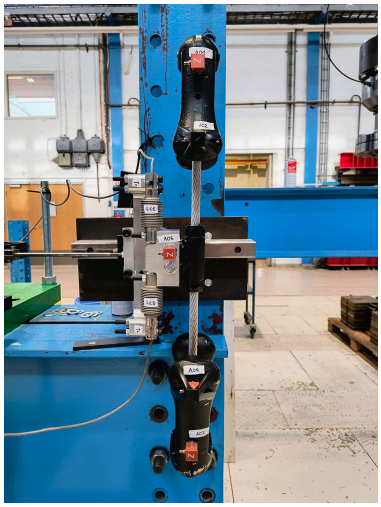

Figure 1. Experimental setup for the whole damper configuration.

2. EXPERIMENTAL DATA

2.1. Impedance function

The impedance function is defined as $Z(\omega) = \frac{F_c(\omega)}{\dot{Y}_c(\omega)}$, where $F_c(\omega)$ is the Fourier transform of the force at the clamp and $\dot{Y}_c(\omega)$ is the Fourier transform of the velocity of the clamp $\dot{y}_c(t)$. Fig. 2 shows impedance functions for the entire damper configuration at various vibration amplitudes. Since the damper dissipates energy through the deformation of the messenger cable, its performance depends on the vibration amplitude. The plot reveals four resonance peaks, which correspond to two degrees of freedom for each mass: lateral oscillation and rotation. Due to the damper's asymmetry, these peaks appear at four distinct frequencies. The wider the amplitude of vibration the more the resonance peaks get sharper and move to lower frequencies.

2.2. Modes of vibration

By analyzing the time history of the mass displacements, it is possible to better understand the two primary vibration modes and the transitions between them. Note that, although these are referred to as "modes of vibration," unique vibration modes cannot be clearly identified due to the system's highly nonlinear nature. To visualize the kind of motion in function of frequency a frequency response function (FRF) can be defined as $H(\omega) = Y_a(\omega)/Y_c(\omega)$, where $Y_a(\omega)$ and $Y_c(\omega)$ are respectively the Fourier transforms of the displacement of a measurement point on the mass and of the clamp displacement. Fig. 4 shows the magnitude of $H(\omega)$ in function of frequency for two points on each mass. The points analyzed are the tip of the messenger cable, measured by sensor $A03$ in Fig. 5b and $A01$ in Fig. 5a, and the outermost point of the mass, measured by sensor $A04$ in

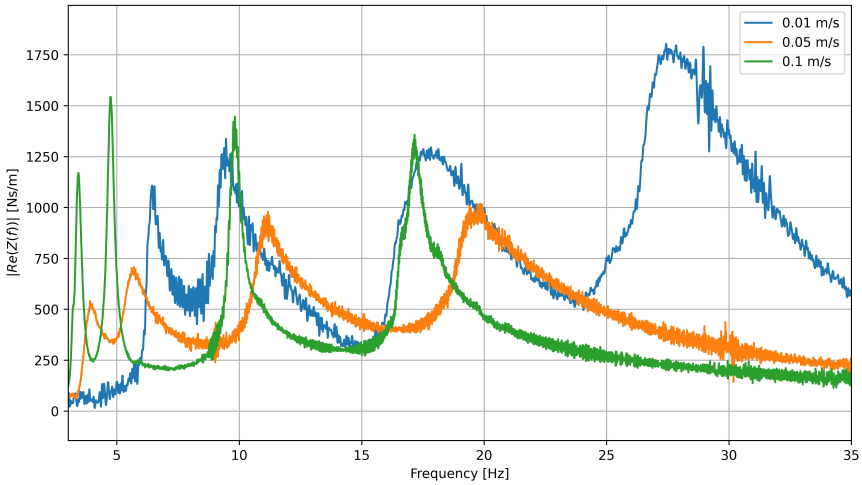

Figure 2. Impedance function of the whole damper for different velocity amplitudes.

Fig. 5b and $A02$ in Fig. 5a. As shown in the plot, for both cases the top sensor moves more at lower frequencies, with the second sensor closely following. In this frequency range, the mass primarily undergoes lateral movement with minimal rotation. A qualitative representation of this mode is given on the left of Fig. 3. At higher frequency, however, there is a reversal: the motion of the outer sensor decreases significantly, while the second sensor registers a peak. This second mode is characterized by minimal lateral translation and a pronounced rotation of the mass about its center of mass, as shown on the right of Fig. 3. Furthermore, it can be noticed how the lower mass (bigger mass) is characterized bby higher and sharper peaks, while the top mass (smaller mass) has lower and wider peaks that cover the entire tested frequency range.

3. CONCLUSIONS

These preliminary results provide insight into the dynamic behavior of the damper. The damper's asymmetry produces three distinct peaks in the system's impedance function. Testing each half separately clarifies the vibration modes, showing that the mass and weight orientation affect not only the resonance frequencies but also the width of the peaks. Notably, the rotational mode peaks differ between the half-damper and whole-damper tests.

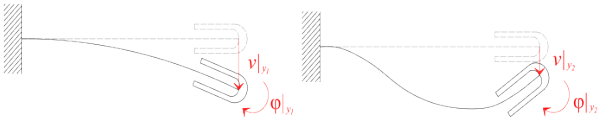

Figure 3. Qualitative representation of the two main modal deformation of half damper (Bogani and Alex, 2021).

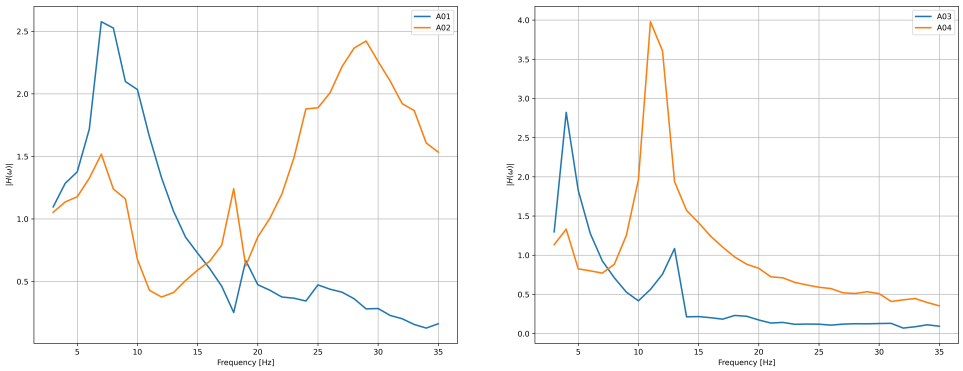

(a) **(b)**

Figure 4. Magnitude of displacement transfer function $H(\omega)$ for damper's a) top half, b) bottom half. Velocity amplitude 0.05m/s.

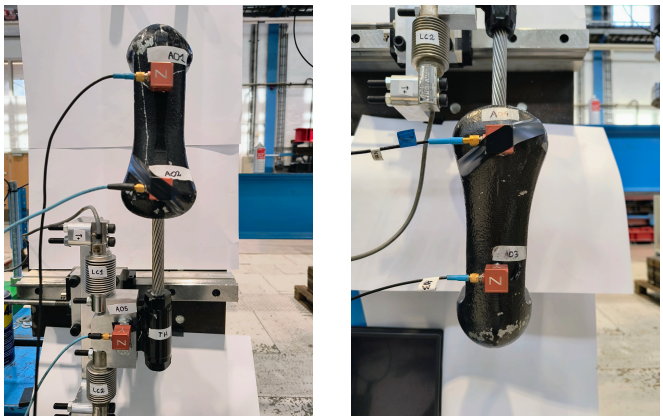

(a) **(b)**

Figure 5. a) Top half of the damper (smaller mass) tested separately. b) Bottom half of the damper (bigger mass) tested separately.

REFERENCES

Barbieri, N. and Barbieri, R., 2012. Dynamic analysis of stockbridge damper. Advances in Acoustics and Vibration 2012.

Bogani, F. and Alex, S., 2021. Modellazione di dissipatori stockbridge per la mitigazione delle vibrazioni eoliche dei cavi sospesi. mathesis, Politecnico di Milano, p. 140.

Foti, F. and Martinelli, L., 2018. Hysteretic Behaviour of Stockbridge Dampers: Modelling and Parameter Identification. Mathematical Problems in Engineering 2018.

IEEE Standards Committee, 1993. IEEE Guide for Laboratory Measurement of the Power Dissipation Characteristics of Aeolian Vibration Dampers for Single Conductors.